Journal of Alloys and Compounds 509 (2011) 8958–8964

Contents lists available at ScienceDirect

Journal of Alloys and Compounds

journal homepage: www.elsevier.com/locate/jallcom

Comparison of hydrogen cycling kinetics in $NaAlH_4$–carbon aerogel composites synthesized by melt infusion or ball milling

F.E. Pinkerton*

Chemical Sciences and Materials Systems Laboratory, General Motors Research and Development Center, MC 480-106-224, 30500 Mound Road, Warren, MI 48090-9055, United States

ARTICLE INFO

Article history:
Received 20 January 2011
Received in revised form 21 June 2011
Accepted 22 June 2011
Available online 29 June 2011

Keywords:
Alanate
Composite materials
Hydrogen absorbing materials
Nanostructured materials
Mechanical alloying
Kinetics

ABSTRACT

This work compares the initial desorption and hydrogen cycling kinetics of $NaAlH_4$ melt infused into carbon aerogel with $NaAlH_4$–carbon aerogel composite synthesized by ball milling. Samples having comparable carbon content (47.4 wt%) prepared by either method yield virtually identical desorption and cycling behavior. Furthermore, the ball milled material can be made with lower carbon content and still maintain only slightly reduced kinetic improvements. Surprisingly, there is no evidence for mixed infused-like and bulk-like behavior even for carbon content as low as 9.1 wt%. Unlike melt infused $NaAlH_4$, where co-infusion of $TiCl_3$ catalyst has proven difficult, the ball milled material can easily accommodate co-doping with both carbon and $TiCl_3$. The inclusion of carbon with $TiCl_3$ results in a modest but significant improvement in kinetics compared to $NaAlH_4$ doped with $TiCl_3$ alone, especially for rehydrogenation. Ball milling with activated carbon produces an improvement very similar to that of carbon aerogel, whereas graphene and graphite have smaller effects, in that order. During cycling of the second stage $NaAlH_4$ reaction, i.e., $Na_3AlH_6 \leftrightarrow 3NaH + Al + (3/2)H_2$, addition of either activated carbon or carbon aerogel at 23.1 wt%, but without $TiCl_3$, results in kinetic performance as good as or better than $NaAlH_4$ doped with $TiCl_3$.

1. Introduction

Complex hydrides are attractive candidates for solid state hydrogen storage in large part because they have high volumetric hydrogen densities (50–115 g hydrogen/l), substantially higher than that offered by compressed H_2 gas (36.7 g H_2/l at 700 bar) [1]. Complex hydrides are also among the solid materials having the highest gravimetric hydrogen densities (for example, 5.6 wt% for $NaAlH_4$ and 13.8 wt% for $LiBH_4$). One of the impediments to their application for on-vehicle hydrogen storage, however, is that hydrogen release is accompanied by phase separation, which limits their absorption and desorption kinetics. Hydrogen release and reabsorption requires bulk diffusion not only of hydrogen but also of the heavier metallic elements in order to accomplish phase separation and recombination.

Sodium alanate ($NaAlH_4$) has been extensively studied as a solid hydride material for on-vehicle hydrogen storage [2–7] and thus serves well as a model system for investigating means to improve kinetics. $NaAlH_4$ reversibly releases hydrogen in two reactions:

$$NaAlH_4 \leftrightarrow (1/3)Na_3AlH_6 + (2/3)Al + H_2 \quad (3.7\,wt\%) \qquad (1)$$

$$(1/3)Na_3AlH_6 + (2/3)Al \leftrightarrow NaH + Al + (1/2)H_2 \quad (1.9\,wt\%) \qquad (2)$$

The overall reaction gives off $(3/2)H_2$ per $NaAlH_4$ with a total hydrogen storage capacity of 5.6 wt%. The two steps are characterized by hydrogenation enthalpies of $\Delta H_d = -37$ kJ/mol H_2 (with corresponding equilibrium temperature under 1 bar of H_2 gas $T_{1\,bar} = 30\,^\circ C$) and -47 kJ/mol H_2 ($T_{1\,bar} = 100\,^\circ C$), respectively. While these hydrogen release reactions are thermodynamically allowed at relatively low temperatures compared to many other complex hydrides, the reaction kinetics of unmodified $NaAlH_4$ are quite slow. In fact, uncatalyzed bulk $NaAlH_4$ generally does not release hydrogen until reaching temperatures well above melting ($T_m = 183\,^\circ C$), and does not readily reabsorb hydrogen under laboratory H_2 pressures and temperatures [2,8]. A decade ago Bogdanović et al. discovered that doping $NaAlH_4$ with titanium, accompanied by nanoscale fabrication (for example by ball milling), reduced the dehydrogenation temperature to below the melting temperature and improved the kinetics of dehydrogenation and rehydrogenation to practical values [2]. The international research effort stimulated by this early work has made $NaAlH_4$ the most thoroughly scrutinized complex hydride for hydrogen storage [9].

Another approach explored by a number of investigators has been the addition of carbon in various forms (graphite, activated carbon, carbon nanofibers, carbon nanotubes, or C_{60} fullerene), either alone or as a co-dopant with Ti [10–23]. It is generally concluded that carbon additions improve the kinetics of $NaAlH_4$,

* Tel.: +1 586 986 0661; fax: +1 586 986 3091.
E-mail address: frederick.e.pinkerton@gm.com

0925-8388/$ – see front matter © 2011 Elsevier B.V. All rights reserved.
doi:10.1016/j.jallcom.2011.06.097

and even Ti-catalyzed $NaAlH_4$ shows modest improvement when co-doped with carbon. Even catalytic levels (~2 wt%) of carbon additions appear to improve the kinetics of $NaAlH_4$ both with [11] and without [13] Ti co-doping. There is little agreement in the literature, however, about which forms of carbon are most efficacious. For example, Wang et al. [14] examined 10 wt% additions of various carbons to $NaAlH_4$ and concluded that activated carbon and graphite were inactive unless co-doped with Ti, while Zaluska et al. [10] found graphite and activated carbon to be equally effective in improving kinetics in the absence of Ti. Berseth et al. [17] similarly found carbon nanotubes, graphite, and C_{60} at 10 wt% addition to be effective dopants in the absence of a catalyst, with C_{60} giving the largest kinetic improvement. More recently, though, it has been shown by the same group [24] that a C_{60}-enriched $NaAlH_4$:C_{60} = 6:1 mixture (69 wt% C_{60}) formed Na_6C_{60} upon thermal dehydrogenation, with the Na embedded within fullerene cages; 1.5 wt% rehydrogenation is attributed in this case to uptake by the $Na@C_{60}$ rather than reforming the $NaAlH_4$. Recent reviews [25,26] summarize the effect of various carbon morphologies on the kinetics of $NaAlH_4$ and other hydride materials, and emphasize that non-planar carbon surfaces such as are found in nanotubes and C_{60} may play an important role by enhancing electron affinity [17,25].

More recently, kinetic improvement has been reported through confinement of $NaAlH_4$ in nanoporous scaffolds. The concept is to constrain phase separation to nanometer dimensions within the pores and thus facilitate recombination [27–33]. For example, by melt infusing $NaAlH_4$ into a carbon aerogel with a pore size distribution peaked near 13 nm, Stephens et al. [34] achieved kinetics rivaling that of Ti-catalyzed $NaAlH_4$ and demonstrated fully reversible hydrogen storage, even though there was no Ti catalyst in the sample. The quantity of $NaAlH_4$ infused, however, was limited by the internal pore volume of the aerogel (0.8 g/cm^3), and amounted to just over half of the sample by weight. Similar results have been reported by de Jongh and co-workers [35–37] for $NaAlH_4$ infused into nanoporous carbon, but with an $NaAlH_4$ loading of only 20 wt% of the sample. They also found, however, that the predominantly 2–3 nm pore size produced a change in the thermodynamics of $NaAlH_4$ dehydrogenation. Altered thermodynamic behavior was also observed by Lohstroh et al. [38] for 48 wt% $NaAlH_4$ melt-infused into activated carbon nanofiber having a preponderance of pores below 4 nm. Baldé et al. [39,40] used solvent impregnation to load 2–9 wt% $NaAlH_4$ into carbon nanofiber bundles and found a factor of two improvement in activation energy in the lowest loading (2 wt% $NaAlH_4$) with $NaAlH_4$ particle sizes limited to 2–10 nm compared to bulk $NaAlH_4$. By solvent infusing $NaAlH_4$ within 2 nm diameter carbon nanotubes, Christian and Aguey-Zinsou [41] were able to observe slight dehydrogenation at room temperature, and heating produced a small release that peaked at 60 °C followed by a much larger broad release extending from 100 to 400 °C. Once again, however, the $NaAlH_4$ loading was quite low, less than 6 wt%. While all of these results are promising, the limited $NaAlH_4$ loading presents a serious impediment to practical application, and research efforts continue to try to increase carbon scaffold pore volumes to improve $NaAlH_4$ loading. Nanoconfinement is an active and growing area of investigation for $NaAlH_4$ as well as other hydrides and hydride systems [25,42,43].

It is therefore of interest to compare the effect on $NaAlH_4$ kinetics of melt infusion into carbon aerogel with alternative processing where similar forms of carbon are intimately mixed with the $NaAlH_4$ simply by ball milling. Here the effect of carbon introduced by melt infusion into carbon aerogel is compared with the effect of ball milling $NaAlH_4$ with the same carbon aerogel, and it is found that either melt infusion or ball milling provide comparable improvement to the dehydrogenation kinetics and the reversibility of reaction (2). The impacts of various forms of carbon, namely, carbon aerogel, activated carbon, graphite, and graphene, are also compared, and it is shown that carbon additions generally improve the cycling kinetics and reversibility of $NaAlH_4$, with or without Ti catalyst, and that mesoporous or microporous carbons (e.g., carbon aerogel or activated carbon) produce the greatest kinetic improvement.

2. Experimental details

$NaAlH_4$ was purchased from Albermarle and used without further purification, as powder X-ray diffraction (XRD) and thermogravimetric analysis (TGA) indicated

Table 1
Summary of sample compositions and kinetic properties.

Carbon	C content (wt%)	$TiCl_3$ content (mol%)[a]	1st desorption midpoint T[b] (°C)	3rd desorption midpoint T (°C)	1st absorption capacity[c] (wt%)	1st absorption time to 50%[d] (min)
None	0	0	278	*>240*[e]	0.77	*>239*[e]
	0	3	(R1) 139			
			(R2) 192	196	1.69	43
$NaAlH_4$@aerogel	~47	0	191	179	2.00	34
Carbon	47.4	0	192	179	2.23	36
aerogel	23.1	0	203	193	2.06	49
	23.1	3	(R1) 135			
			(R2) 189	[f]	1.85	37
Activated	23.1	0	205	203	2.13	68
carbon	16.7	0	219	208	2.01	80
	9.1	0	228	*>213*[e]	1.77	*>140*[e]
	23.1	3	(R1) 134			
			(R2) 188	185	1.77	37
Graphene	23.1	0	245	*>227*[e]	1.30	*>247*[e]
Graphite	23.1	0	265	*>233*[e]	0.93	*>247*[e]

[a] Relative to $NaAlH_4$ content.
[b] Temperature at which the desorption reached 50% of that sample's total capacity. The two different desorption reactions (R1) and (R2), could be resolved only in the Ti-catalyzed samples.
[c] Capacity after 12 h of hydrogenation at 140 °C in 19.8 bar H_2.
[d] Time to reach 1/2 of the final absorption capacity during hydrogenation. Time is measured from the start of heating, and includes roughly 30 min for the temperature to reach 140 °C.
[e] Samples did not approach full capacity during the first and subsequent 12 h absorptions. The values in italics are thus lower bounds for the actual times to reach half of full capacity.
[f] Experiment terminated abnormally after the second desorption.

no significant contaminants (see Supporting Information). $TiCl_3$ (Aldrich, 99.999%) was used for Ti-catalyzed samples. Carbon additives included commercial graphite (Alfa, 99.5%), activated carbon (Alfa Aesar, max. 4% ash), and graphene (XG Sciences xGnP 5 μm). In addition, carbon aerogel cubes having a 13 nm average pore size provided by HRL Laboratories, LLC were used either as a carbon additive or as a scaffold for melt infusion of $NaAlH_4$. Sorbed water was removed from the carbon starting materials by heating under vacuum.

Samples of $NaAlH_4$ containing X wt% carbon additive (X = 9.1, 16.7, 23.1, or 47.4) were prepared by mixing the desired quantities of $NaAlH_4$ powder and carbon and ball milling for 1 h in a SPEX Model 8000 Mixer/Mill with one large and two small balls in a round-ended hardened steel vial. Most of the samples examined in this work contained 23.1 wt% carbon. For activated carbon, the carbon content was varied from X = 9.1 to 23.1 wt%. For the HRL carbon aerogel, samples were made at both 23.1 wt% and 47.4 wt%; the latter approximates the composition of samples made by melt-infusing $NaAlH_4$ into 13 nm carbon aerogel [34]. Catalyzed ball milled samples were made in the case of pure $NaAlH_4$, activated carbon, and HRL aerogel by including 0.03 mol of $TiCl_3$ per mole of $NaAlH_4$. All samples were handled and ball mill vials were loaded inside of an Ar inert gas glove box to prevent atmospheric contamination. Chemical analysis using Inductively Coupled Plasma Atomic Emission Spectrometry (ICP/AES) was performed on representative ball milled samples to check for contamination by Fe from the ball milling process. In all cases the Fe content was 0.08 wt% or lower, far too low to act as an effective catalyst. A summary of samples is provided in Table 1.

For comparison $NaAlH_4$ was melt-infused into HRL carbon aerogel (hereafter designated $NaAlH_4$@aerogel) by placing a cube of aerogel weighting 0.2590 g into a quartz bucket and covering the cube with 0.2866 g of $NaAlH_4$ powder. This weight ratio of $NaAlH_4$ to aerogel represents a 10% excess of $NaAlH_4$ relative to the amount estimated to just fill the pore volume in the aerogel. The quartz bucket was sealed in the glove box into a PARR high pressure reactor, which was then removed from the glove box and transported to a heating sleeve. The vessel was charged with 163 bar of H_2 gas at room temperature, and then gradually heated to 204 °C, a temperature slightly above the melting temperature of $NaAlH_4$ (183 °C). At this temperature the H_2 pressure was 278 bar, sufficient to prevent the molten $NaAlH_4$ from dehydrogenating. The vessel was held at this temperature for 250 min, then cooled to room temperature, depressurized, and purged with He to remove the remaining H_2. The vessel was returned to the glove box and the infused aerogel removed in the form of partially decrepitated shards.

XRD results were obtained by loading the powder into 1 mm inner diameter capillary tubes inside the glove box and sealing with clay. The capillaries were transported to a Bruker AXS X-ray diffractometer equipped with a General Area Detector Diffraction System (GADDS).

Initial dehydrogenation and hydrogen cycling were performed in a Hiden Model IGA-3 thermogravimetric analyzer. Dehydrogenations were performed under 1 bar of He gas flowing at 200 ml/min while heating the sample at 4.3 °C/min to the target temperature. The sample was held at the target temperature for about 20 min before cooling back to room temperature. The target temperature varied with sample because further decomposition of NaH to Na and hydrogen gas, which normally occurs only well in excess of 300 °C, can be catalyzed by carbon to occur at substantially reduced temperatures [18]. The maximum temperature for a given form of carbon was selected to be just sufficient to complete reaction (2), the decomposition of Na_3AlH_6, and minimize higher temperature exposure that might further decompose the NaH (see below). Hydrogenations were conducted in 19.8 bar of H_2 gas flowing at 200 ml/min. The temperature was ramped at 4.3 °C/min to 140 °C and held for 12 h. The temperature profile was nearly identical for all samples. Between each half-cycle, the sample was cooled to room temperature, depressurized to vacuum, and repressurized with the appropriate gas. Three dehydrogenation–rehydrogenation cycles were performed on each sample. Although the limited number of cycles does not address long term stability, the reproducibility over three cycles ensures that there are no gross changes in the samples during cycling, especially during the initial dehydrogenation and rehydrogenation. In contrast, ball milled $TiCl_3$-catalyzed $NaAlH_4$ can show significant differences between the first and subsequent cycles, see for example Stephens et al. [34].

Because the H_2 pressure was limited in the Hiden apparatus to <20 bar, only reaction (2) could occur, reforming Na_3AlH_6 from NaH and Al. Cycling observations were thus limited to reaction (2). Following the results of Zaluska et al. [10], some kinetic improvement is expected also for reaction (1); results for initial dehydrogenation support this conjecture. To test for reaction (1) acceleration, one sample, $NaAlH_4$ + 23.1 wt% carbon aerogel, was cycled in an alternate apparatus (Cahn Model 2151 high pressure TGA) using 96 bar hydrogenations.

3. Results and discussion

3.1. Comparison of ball milled and melt infused $NaAlH_4$–carbon aerogel

Uncatalyzed $NaAlH_4$ ball milled with HRL carbon aerogel is compared in Fig. 1 with $NaAlH_4$ that has been melt infused into carbon aerogel ($NaAlH_4$@aerogel). Two levels of aerogel addition are shown, 23.1 wt% (dark blue) and 47.4 wt% (orange). The latter composition was chosen to provide approximately the same amount of carbon as is contained in the $NaAlH_4$@aerogel sample (green). For completeness the dehydrogenation of ball milled $NaAlH_4$ without carbon is also shown (black). All desorption amounts are given relative to the $NaAlH_4$ content in the sample for purposes of comparison. The ball milled and melt infused samples having about the same carbon level (X = 47.4 wt%) released hydrogen at about the same temperature; the midpoints of desorption differed by only about 1 °C, which is within experimental error. Two differences are apparent in the ball milled material: first, there was a small but significant weight loss even at temperatures below 100 °C, and second, the amount of hydrogen desorbed was higher. The relatively lower amount of hydrogen released from the melt infused sample may be due to the infusion being not quite complete. The total weight loss from the ball milled sample actually exceeded the theoretical capacity of the total of reactions (1) and (2) due to slight decomposition of NaH to Na [18], as discussed in Section 2.

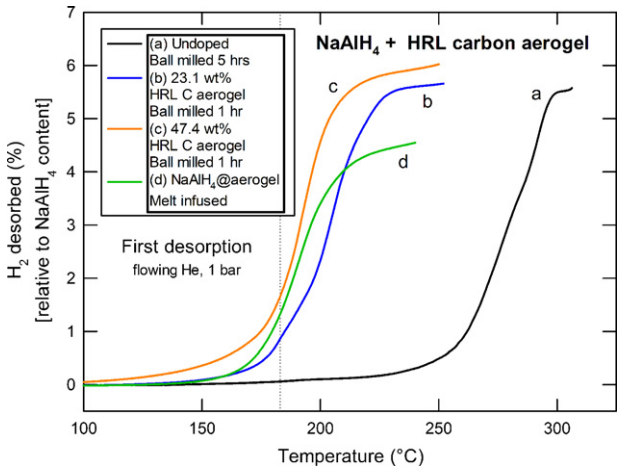

Fig. 1. Initial desorption of $NaAlH_4$ samples with HRL carbon aerogel prepared by melt infusion or by ball milling. The ball milled sample with 47.4 wt% aerogel is comparable in carbon content to the $NaAlH_4$@aerogel sample. The 23.1 wt% aerogel sample has insufficient pore volume to accommodate all of the $NaAlH_4$ by about a factor of three. The dotted vertical line shows the melting temperature of bulk $NaAlH_4$.

Dehydrogenation of the ball milled sample with 23.1 wt% aerogel occurred at only slightly higher temperature (by 11 °C), and was still reduced by 75 °C compared to undoped $NaAlH_4$. Essentially full capacity weight loss was observed by 230 °C. Its behavior was very similar to the melt infused sample, albeit at slightly higher temperature, in spite of the fact that at this additive level the pore volume of the aerogel was insufficient to hold all of the $NaAlH_4$. Indeed, from previous estimates the internal volume of the aerogel was only sufficient to hold about 30% of the $NaAlH_4$, while the remaining 70%, at a minimum, must be outside of the aerogel. Curiously, there was no evidence for the mixed behavior that might be expected from such a sample, i.e., having 30% of the weight loss follow the behavior of the infused sample, and the other 70% remaining bulk-like (following the black curve). Instead, there was a single, continuous behavior only shifted a bit from the fully infused case. This point will be discussed further below.

Similar results were obtained for the first rehydrogenation in 19.8 bar H_2 pressure at 140 °C, as shown in Fig. 2. As previously stated, under this pressure–temperature condition, only reaction (2) was reversible. The undoped decomposed $NaAlH_4$ absorbed only 0.77 wt% hydrogen even after 12 h of exposure. In contrast, the aerogel-containing samples all readily reabsorbed hydrogen. There was again little difference between the melt-infused and

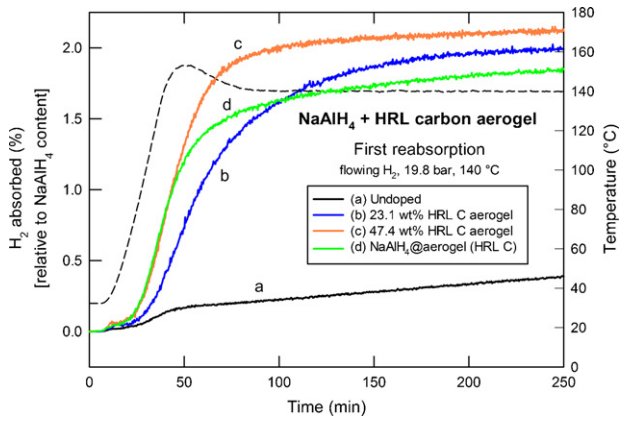

Fig. 2. First reabsorption for the same four samples as in Fig. 1, again illustrating the similarity between melt infused and ball milled samples. Only reaction (2) is reversible under the experimental temperature and pressure conditions. Undoped $NaAlH_4$ rehydrogenates poorly. The dashed curve is the temperature profile.

the ball milled samples at $X = 47.4$ wt%, except that once again the ball milled sample showed better capacity. In fact, as was the case in desorption, the ball milled sample actually exceeded the theoretical capacity for reaction (2). This is consistent with the presence of a small quantity of Na in the dehydrogenated sample that rehydrogenates under these conditions, eventually forming the intermediate hexahydride.

Subsequent dehydrogenation via reaction (2) is presented in Fig. 3. The similarity of the melt infused and ball milled materials was once again evident, as was the greatly enhanced performance of the 23.1 wt% aerogel ball milled sample.

Upon cycling, there was very little additional change except for a general decrease in the cycling capacity (see Supporting Information). The amount was sample dependent, but ranged from 1% to as high as 27% capacity reduction after the third rehydrogenation. This diminution is attributed to gradual oxidation of the sample by impurities in the gas flow, which accumulated to significant values because of the long hydrogenation times and the repeated evacuations and backfills in the experimental protocol. The 27% value in particular was an early sample that experienced relatively long idle times between cycles, before the importance of this effect was recognized.

When rehydrogenated at 96 bar, improved kinetics are also observed for dehydrogenation and rehydrogenation of reaction (1) (see Supporting Information). The reaction (1) reabsorption, however, is slower than that of the reaction (2) reabsorption, and is not complete even after 12 h.

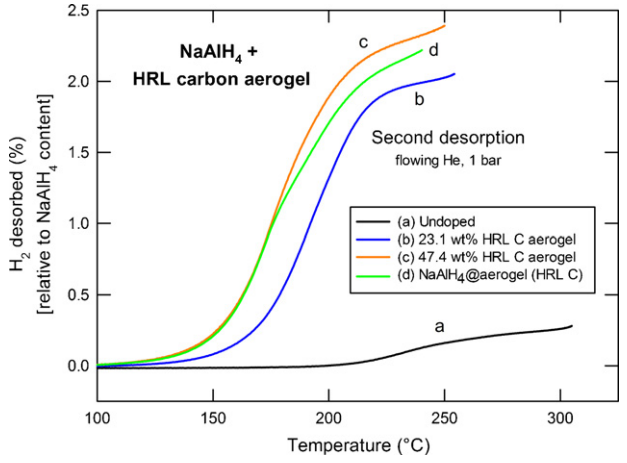

Fig. 3. Reaction (2) second cycle desorption of the same four samples as Fig. 1.

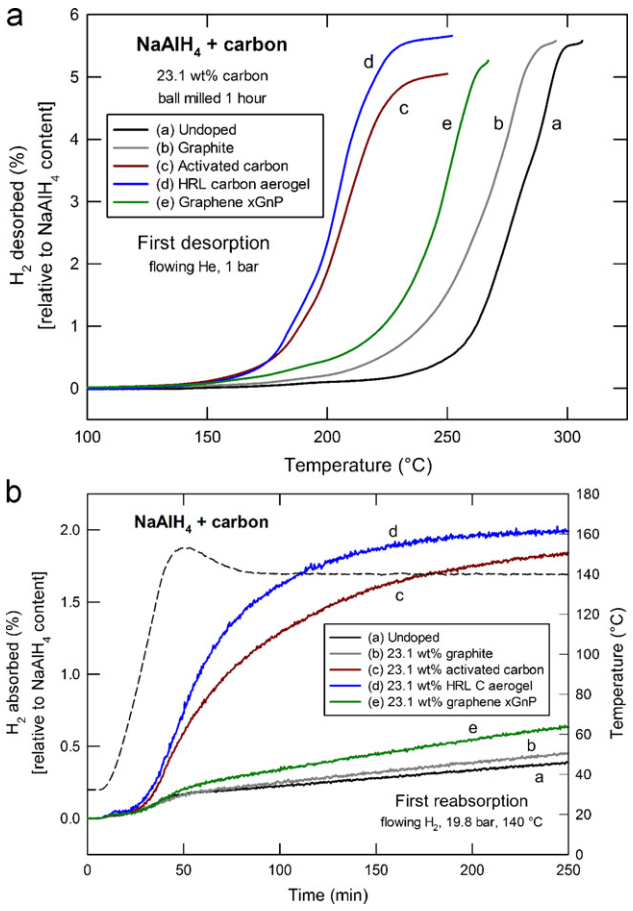

Fig. 4. Initial desorption (a) and subsequent first reabsorption (b) comparing various forms of carbon at 23.1 wt% addition.

3.2. *Effect of different carbon morphologies*

Fig. 4(a) compares the effect of several different forms of carbon on the initial desorption of $NaAlH_4$ at 23.1 wt% loading. Except for a small difference in capacity, activated carbon gave results nearly identical to the ball milled HRL carbon aerogel. Correspondingly smaller improvements in dehydrogenation temperature were observed for graphene and graphite. On rehydrogenation (Fig. 4(b)) the graphite and graphene samples showed only incomplete rehydrogenation, although the amount of hydrogen reabsorbed in 12 h was qualitatively consistent with changes in the initial dehydrogenation temperature. Once again, the activated carbon sample was nearly the same as the carbon aerogel when ball milled. Curiously, by the third cycle the midpoint of dehydrogenation for most of the carbon samples had decreased by about 10 °C; the rehydrogenation curves, however, remained virtually identical. These results are different from those reported by Zaluska et al. [10], in that graphite and activated carbon do not give about the same improvement, but rather graphite is minimally active while activated carbon is highly beneficial. They also contradict Wang et al. [14], who reported that carbons, including activated carbon, were inactive unless Ti was present.

The carbon aerogel has a broad pore size distribution centered near 13 nm, whereas the activated carbon pore size distribution increases smoothly with decreasing pore size and exhibits a substantial microporous tail below 2 nm (see Supporting Information). The aerogel and activated carbon nevertheless have very similar

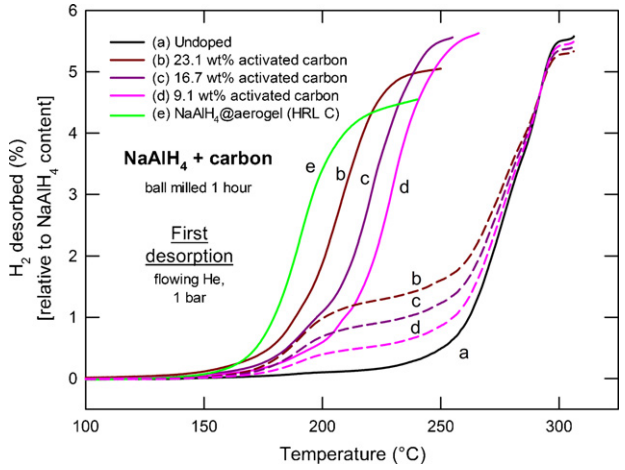

Fig. 5. Initial desorption for $NaAlH_4$ samples with varying activated carbon loading, compared to a melt-infused sample and undoped $NaAlH_4$. The dashed curves represent the expected desorption if the samples behave like a weighted superposition of an infused-like and a bulk-like component.

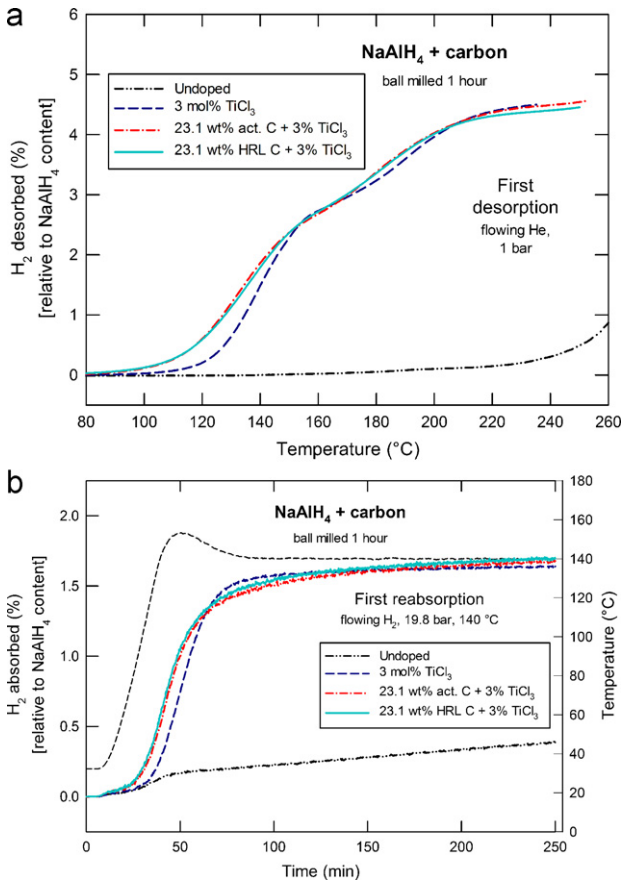

Fig. 6. Initial desorption (a) and subsequent first reabsorption (b) of $NaAlH_4$ with 3 mol% $TiCl_3$ added as a catalyst, without and with co-doping by 23.1 wt% activated carbon or HRL carbon aerogel.

BET specific surface areas (750 and 940 m^2/g, respectively) and total pore volumes (0.84 and 0.71 cm^3/g, respectively). These similarities seem to yield comparable kinetic improvement irrespective of the actual pore size distributions.

One possible explanation for the enhanced kinetics in the aerogel and activated carbon samples is that the alanate melted and infused into the pores of the carbon during the first desorption heating. While plausible, further examination shows that this cannot be the dominant source of improved kinetics. Initial desorption is shown in Fig. 5 for several different loadings of activated carbon. When the quantity of activated carbon was decreased from 23.1 to 9.1 wt%, desorption still occurred virtually as a single step. At 9.1 wt% activated carbon, there was only enough pore volume in the carbon to hold about 9% of the $NaAlH_4$ in the sample. If the improved kinetics were due solely to infusion, it should give a weighted superposition of bulk-like desorption and melt infused desorption, as suggested by the corresponding dashed curve in Fig. 5. Instead a single continuous behavior was observed, shifted to higher temperature by 38 °C. Even at 23.1 wt% carbon, only about a quarter of the $NaAlH_4$ could fit into the activated carbon pore volume. Furthermore, a substantial fraction of the hydrogen was desorbed below the $NaAlH_4$ melting temperature. Finally, large kinetic enhancement was also observed during reabsorption (see Supporting Information) even when only a small fraction of the $NaAlH_4$ decomposition products could be within pores. There are small inflection points on the desorption curves which are suggestive of infused-like behavior, however the major temperature reduction compared to undoped material affected the entire sample, an observation not consistent with infusion as the primary origin.

The dehydrogenation curves displayed in Fig. 5 are corroborated by very recent results from Lin et al. [22] on $NaAlH_4$ with 10 wt% and 30 wt% activated carbon additions. They observed hydrogen releases during heating that closely resemble the 9.1 wt% and 23.1 wt% samples, respectively. Perhaps because their magnitudes of the hydrogen release are not quantified, they attribute the improved kinetics to melt infusion during heating; however, the full dehydrogenations shown in Fig. 5 are not consistent with such a conclusion, as discussed above.

The effects of nanoporous carbon on the kinetics of reaction (2) in ball milled materials share many of the characteristics of catalysts: relatively small quantities of carbon have a large effect; as the amount of carbon increases the kinetics continue to improve but at a rate slower than linear; and high surface area appears to be crucial. Adelhelm and de Jongh [26] concluded that carbon plays multiple roles in affecting kinetics of $NaAlH_4$, and includes a direct interaction beyond the nanosize effects of confinement and hindering grain growth during cycling of nanoparticle hydrides. The dependence of kinetics on carbon content supports this conclusion. That graphite and graphene also show some kinetic improvement, albeit modest, also argues for a non-nanoscale effect from carbon, as does preliminary electron microscopy examination indicating that the carbon aerogel particles in ball milled samples range in size from 100 nm to 1 μm, and hence are not truly nanodispersed. The reduced impact of graphite and graphene may be due in part to the preponderance of planer carbon surfaces in these materials, compared to the irregular carbon surfaces in nanoporous morphologies [17,25]. Further study is needed to fully resolve the interplay between nanoporous carbon particles and $NaAlH_4$.

3.3. *Incorporation of $TiCl_3$ catalyst*

It has been well established that addition of a few mole percent of a transition metal such as Ti (typically introduced via Ti butoxide or a metal salt) greatly improves the kinetics of $NaAlH_4$. Indeed, it was this observation by Bogdanović et al. [2] that led to extensive study of $NaAlH_4$ as a hydrogen storage material. It is thus of interest to examine the impact of co-doping carbon and Ti in $NaAlH_4$. In this work, Ti was introduced into the $NaAlH_4$ powder by ball milling a mixture of $NaAlH_4$ with 3 mol% $TiCl_3$. Fig. 6(a) shows the effect of adding 3 mol% $TiCl_3$ on the initial desorption of $NaAlH_4$ (dark blue curve). Also shown are desorptions for samples in which $NaAlH_4$ has been co-milled with 3 mol% $TiCl_3$ (relative to the $NaAlH_4$ con-

tent) and 23.1 wt% carbon in the form of either activated carbon (red) or carbon aerogel (light blue). Although the effect of carbon on $TiCl_3$-doped $NaAlH_4$ was much less dramatic than those described above for Ti-free $NaAlH_4$, nevertheless carbon addition did improve the kinetic performance significantly compared to $TiCl_3$ alone. The mid-point temperature of the first decomposition step (R1) was shifted to lower temperature by about 5 °C, although early in the decomposition the temperature shift was in excess of 10 °C. In operation this would translate to significantly faster kinetics at a fixed operating temperature. The kinetics of the second step (R2) improved by about 4 °C. For comparison, Lin et al. [22] examined the effect on $NaAlH_4$ kinetics of decorating activated carbon with small quantities of Co, Cu, or Ni particles, and found that decorated carbon worked somewhat better than the carbon alone, but not as well as standard $TiCl_3$-catalyzed $NaAlH_4$. It appears that combining nanoporous carbon with a Ti-based catalyst is more efficacious than carbon with Co, Cu, or Ni metal catalyst particles.

It is worth emphasizing that there are no comparison data presented here for ($NaAlH_4$ + $TiCl_3$)@aerogel, i.e., aerogel that has been infused with Ti-added $NaAlH_4$. To date it has proven intractable to simultaneously melt infuse aerogel with both $NaAlH_4$ and $TiCl_3$. Our attempts at melt-infusion with $NaAlH_4$ loadings corresponding to full pore filling resulted in low yields of infused material, without improvement in the dehydrogenation behavior beyond $NaAlH_4$@aerogel without $TiCl_3$, and certainly not approaching the behavior of $TiCl_3$-added $NaAlH_4$ itself. Recently some success has been achieved in co-incorporation, but only at $NaAlH_4$ loadings well below complete pore filling. Nielsen et al. [44] first solvent infused $TiCl_3$ into a 17 nm carbon aerogel, followed by $NaAlH_4$ melt infusion, but limited the $NaAlH_4$ loading to 33.3 wt%, well below the saturation limit, in order to obtain complete $NaAlH_4$ infiltration. The co-infiltrated aerogel did show substantially improved kinetic performance compared to a ball milled $NaAlH_4$–$TiCl_3$ sample, with the peak hydrogen release occurring about 35 °C lower in temperature. $NaAlH_4$ and $Ti(OBu)_4$ were successively solvent infused to produce catalyzed $NaAlH_4$ supported on carbon nanofibers by Baldé et al. [45], with an 8 wt% $NaAlH_4$ loading.

Co-doping with $TiCl_3$ and carbon also significantly improved rehydrogenation, at least for reaction (2). This is observed in Fig. 6(b), where the carbon-added samples took up hydrogen about 6 min sooner than the $TiCl_3$-only sample during heating to the soak temperature; at the heating rate of 4.3 °C/min this was equivalent to a temperature shift of about 26 °C. Furthermore, reaction (2) was also accelerated by carbon during subsequent desorptions, as illustrated by the second desorption data in Fig. 7. In this case, co-doping with carbon improved the desorption temperature by about 15 °C. Perhaps more surprising are the results also overlaid in Fig. 7 for carbon aerogel, both ball milled and melt infused, without $TiCl_3$. The second desorption was superior for these samples compared to $TiCl_3$-added $NaAlH_4$, even in the absence of Ti.

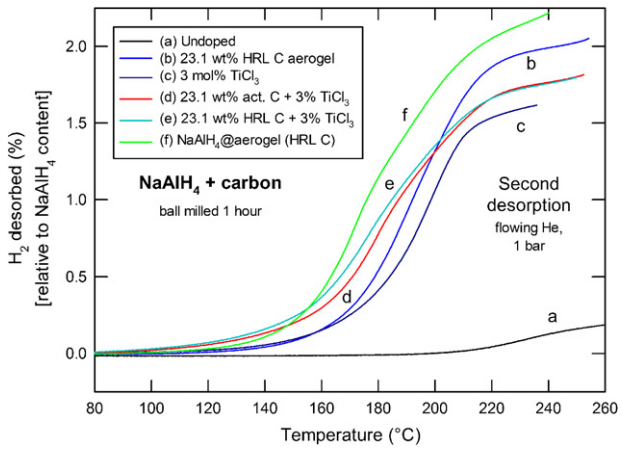

Fig. 7. Second desorption (reaction (2)) for $TiCl_3$-catalyzed $NaAlH_4$ without and with co-doping by 23.1 wt% activated carbon or HRL carbon aerogel. Also shown for comparison are melt-infused or ball milled samples with HRL carbon aerogel, but without $TiCl_3$. These latter two samples are comparable to, or better than, $TiCl_3$-catalyzed $NaAlH_4$, even without the presence of Ti.

Although it is not obvious from the figures presented here because of the normalization to $NaAlH_4$ content, clearly the inclusion of up to 23.1 wt% carbon will reduce the effective hydrogen capacity by dilution. The kinetic improvements of carbon in the $TiCl_3$-added samples are unlikely to be significant enough to justify the lost capacity. However, some forms of carbon at the 10–20 wt% level are candidates for enhancing thermal conductivity when mixed with $NaAlH_4$, and it is significant that an accompanying synergistic improvement in hydrogen cycling kinetics might also be achieved. In fact, Fig. 7 suggests that in the presence of carbon, it may no longer be necessary to also add $TiCl_3$.

4. Conclusions

Incorporating graphite, graphene, activated carbon, and a carbon aerogel at 23.1 wt% into $NaAlH_4$ by ball milling confirms previous observations [10,15,17,19,21–23] that carbon can improve the kinetics of dehydrogenation and cycling of $NaAlH_4$ even in the absence of a transition metal catalyst. In this work graphite had a minimal effect, and graphene was only somewhat better, whereas microporous activated carbon and mesoporous carbon aerogel produced large and essentially equivalent kinetic improvements compared to additive-free $NaAlH_4$. As detailed in Section 1, these results differ from some of the previous reports [10,14]. Notably, addition of 23.1 wt% activated carbon or carbon aerogel produced kinetic improvements to the cycling of reaction (2) ($Na_3AlH_6 \leftrightarrow 3NaH + Al + (3/2)H_2$) that were comparable to that produced by Ti addition, even though Ti was not present. When also catalyzed with $TiCl_3$, activated carbon and carbon aerogel provided more modest, but still significant, improvements to the cycling kinetics.

Results comparable to melt infusion were achieved by simply ball milling aerogel with $NaAlH_4$. Furthermore, both carbon and $TiCl_3$ were successfully incorporated simultaneously into $NaAlH_4$ samples by ball milling, resulting in kinetics superior to $TiCl_3$ additions alone, in general agreement with previous observations [11,12,14–17,20]. Co-incorporation of a Ti catalyst has proven difficult via melt infusion. Ball milling thus provides a more flexible and straightforward preparation technique for sample synthesis.

Ball milling also allows $NaAlH_4$ concentrations substantially higher than the limit imposed by full pore filling in melt infusion or solvent infusion. While reducing the quantity of activated carbon modestly increased the desorption temperature, it still maintained a large improvement over additive-free $NaAlH_4$, and without any appearance of bulk-like behavior even at carbon concentrations as low as 9.1 wt% where no more than about 10% of the $NaAlH_4$ could be located inside carbon pores. Even this relatively low level of activated carbon greatly improved the reversibility of reaction (2). The kinetic improvement is larger than a simple proportionality to the amount of carbon, and there is no sign of mixed behavior. Clearly the kinetic improvement cannot be ascribed solely to nanoscale confinement. Major contribution from a direct catalytic effect of carbon on $NaAlH_4$ and its products is consistent with the observed kinetic improvements, although further study is needed to verify its nature.

The extent to which various carbon morphologies work with other emerging complex hydride materials is an open question. Work is under way to establish the kinetic improvements of ball

milling other complex hydrides with nanoporous carbons, motivated by the improvement demonstrated for melt infused $LiBH_4$ [30].

Acknowledgments

The author thanks John Vajo and Adam Gross of HRL Laboratories, LLC for providing the carbon aerogel sample. I also thank Martin Meyer, Mike Balogh, Curt Wong, and Nick Irish for technical support.

Appendix A. Supplementary data

Supplementary data associated with this article can be found, in the online version, at doi:10.1016/j.jallcom.2011.06.097.

References

[1] J.F. Herbst, F.E. Pinkerton, in: J. Weil, D. Blumel, S. Malmoli, J. Netting (Eds.), McGraw-Hill Yearbook of Science and Technology 2008, McGraw-Hill, New York, 2008, pp. 172–175.
[2] B. Bogdanović, M. Schwickardi, J. Alloys Compd. 253–254 (1997) 1.
[3] B. Bogdanović, R.A. Brand, A. Marjanovic, M. Schwickardi, J. Tölle, J. Alloys Compd. 302 (2000) 36.
[4] C.M. Jensen, K. Gross, Appl. Phys. A 72 (2001) 213.
[5] G. Sandrock, K. Gross, G. Thomas, J. Alloys Compd. 339 (2002) 299.
[6] F. Schüth, B. Bogdanović, M. Felderhoff, Chem. Commun. (2004) 2249.
[7] B. Bogdanović, U. Eberle, M. Felderhoff, F. Schüth, Scr. Mater. 56 (2007) 813.
[8] G.P. Meisner, G.G. Tibbetts, F.E. Pinkerton, C.H. Olk, M.P. Balogh, J. Alloys Compd. 337 (2002) 254.
[9] I.P. Jain, P. Jain, A. Jain, J. Alloys Compd. 503 (2010) 303–339.
[10] A. Zaluska, L. Zaluski, J.O. Ström-Olsen, J. Alloys Compd. 298 (2000) 125.
[11] Z. Dehouche, L. Lafi, N. Grimard, J. Goyette, R. Chahine, Nanotechnology 16 (2005) 402.
[12] J. Wang, A.D. Ebner, T. Prozorov, R. Zidan, J.A. Ritter, J. Alloys Compd. 395 (2005) 252.
[13] D. Pukazhselvan, B.K. Gupta, A. Srivastava, O.N. Srivastava, J. Alloys Compd. 403 (2005) 312.
[14] J. Wang, A.D. Ebner, J.A. Ritter, J. Phys. Chem. B 110 (2006) 17353.
[15] C. Cento, P. Gislon, M. Bilgili, A. Masci, Q. Zheng, P.P. Prosini, J. Alloys Compd. 437 (2007) 360.
[16] Y. Suttisawat, P. Rangsunvigit, B. Kitiyanan, S. Kulprathipanja, Int. J. Hydrogen Energy 33 (2008) 6195.
[17] P.A. Berseth, A.G. Harter, R. Zidan, A. Blomqvist, C.M. Araújo, R.H. Scheicher, R. Ahuja, P. Jena, Nano Lett. 9 (2009) 1501.
[18] P. Adelhelm, K.P. de Jong, P.E. de Jongh, Chem. Commun. (2009) 6261.
[19] D. Lupu, G. Blanita, I. Misan, O. Ardelean, I. Coldea, G. Popeneciu, A.R. Biris, J. Phys. Conf. Ser. 182 (2009) 012050.
[20] Y. Suttisawat, P. Rangsunvigit, B. Kitiyanan, S. Kulprathipanja, J. Solid State Electrochem. 14 (2010) 1813–1819.
[21] H. Raghubanshi, M.S.L. Hudson, O.N. Srivastava, Int. J. Hydrogen Energy 36 (2011) 4482–4490.
[22] S.S.-Y. Lin, J. Yang, H.H. Kung, Int. J. Hydrogen Energy, in press.
[23] M.S.L. Hudson, H. Raghubanshi, D. Pukazhselvan, O.N. Srivatava, Int. J. Hydrogen Energy, in press.
[24] J.A. Teprovich Jr., D.A. Knight, M.S. Wellons, R. Zidan, J. Alloys Compd., in press.
[25] C.Z. Wu, H.M. Cheng, J. Mater. Chem. 20 (2010) 5390–5400.
[26] P. Adelhelm, P.E. de Jongh, J. Mater. Chem. 21 (2011) 2417.
[27] F. Schüth, B. Bogdanović, A. Taguchi, Patent Application WO2005014469 (2003).
[28] A. Gutowska, L. Li, Y. Shin, C.M. Wang, X.S. Li, J.C. Linehan, R.S. Smith, B.D. Kay, B. Schmid, W. Shaw, M. Gutowski, T. Autrey, Angew. Chem. Int. Ed. 44 (2005) 3578.
[29] S. Zheng, F. Fang, G. Zhou, L. Ouyang, M. Zhu, D. Sun, Chem. Mater. 20 (2008) 3954.
[30] A.F. Gross, J.J. Vajo, S.L. Van Atta, G.L. Olson, J. Phys. Chem. C 112 (2008) 5651.
[31] R.K. Bhakta, J.L. Herberg, B. Jacobs, A. Highley, R. Behrens Jr., N.W. Ockwig, J.A. Greathouse, M.D. Allendorf, J. Am. Chem. Soc. 131 (2009) 13198.
[32] P.E. de Jongh, P. Adelhelm, ChemSusChem 3 (2010) 1332.
[33] Y. Li, G. Zhou, F. Fang, X. Yu, Q. Zhang, L. Ouyang, M. Zhu, D. Sun, Acta Mater. 59 (2011) 1829.
[34] R.D. Stephens, A.F. Gross, S.L. Van Atta, J.J. Vajo, F.E. Pinkerton, Nanotechnology 20 (2009) 204018.
[35] J. Gao, P. Adelhelm, M.H.W. Verkuijlen, C. Rongeat, M. Herrich, P.J.M. van Bentum, O. Gutfleisch, A.P.M. Kentgens, K.P. de Jong, P.E. de Jongh, J. Phys. Chem. C 114 (2010) 4675.
[36] M.H.W. Verkuijlen, J. Gao, P. Adelhelm, P.J.M. van Bentum, P.E. de Jongh, A.P.M. Kentgens, J. Phys. Chem. C 114 (2010) 4683.
[37] P. Adelhelm, J. Gao, M.H.W. Verkuijlen, C. Rongeat, M. Herrich, P.J.M. van Bentum, O. Gutfleisch, A.P.M. Kentgens, K.P. de Jong, P.E. de Jongh, Chem. Mater. 22 (2010) 2233.
[38] W. Lohstroh, A. Roth, H. Hahn, M. Fichtner, ChemPhysChem 11 (2010) 789–792.
[39] C.P. Baldé, B.P.C. Hereijgers, J.H. Bitter, K.P. de Jong, Angew. Chem. Int. Ed. 45 (2006) 3501–3503.
[40] C.P. Baldé, B.P.C. Hereijgers, J.H. Bitter, K.P. de Jongh, J. Am. Chem. Soc. 130 (2008) 6761.
[41] M. Christian, K.F. Aguey-Zinsou, Nanoscale 2 (2010) 2587–2590.
[42] T.K. Nielsen, F. Besenbacher, T.R. Jensen, Nanoscale 3 (2011) 2086–2098.
[43] J.J. Vajo, Curr. Opin. Solid State Mater. Sci. 15 (2011) 52–61.
[44] T.K. Nielsen, M. Polanski, D. Zasada, P. Javadian, F. Besenbacher, J. Bystrzycki, J. Skibsted, T.R. Jensen, ACS Nano 5 (2011) 4056–4064.
[45] C.P. Baldé, O. Leynaud, P. Barnes, E. Peláez-Jiménez, K.P. de Jong, J.H. Bitter, Chem. Commun. 47 (2011) 2143–2145.